Article

Cell Reports

Dissecting the Control Mechanisms for DNA Replication and Cell Division in *E. coli*

Graphical Abstract

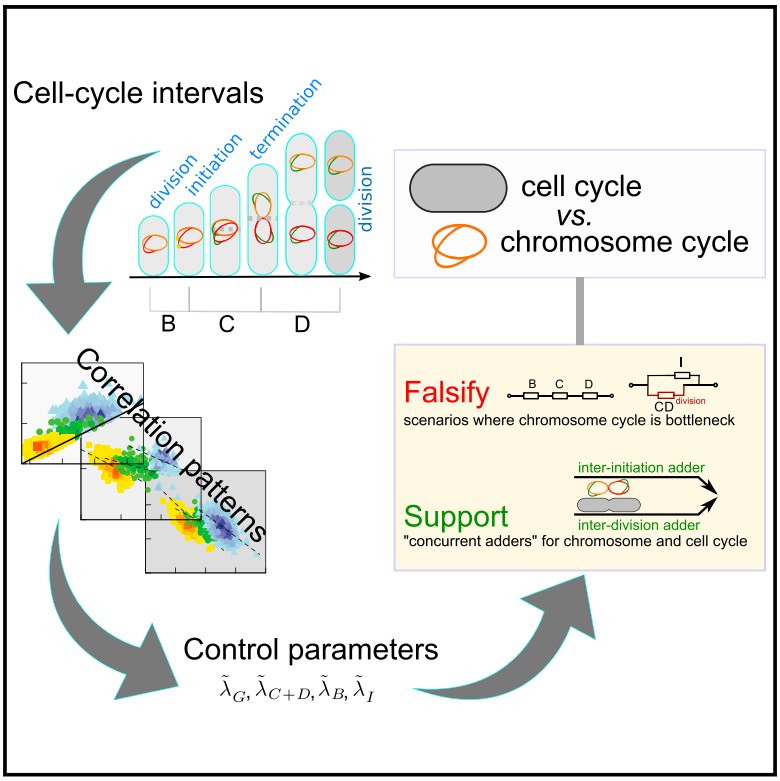

Highlights

- The classic view that genome replication limits cell division fails with data
- Stochastic models based on this hypothesis do not capture single-cell data trends
- A model with concurrent initiation and division processes captures the data
- Concurrent processes add a constant size (adders) between divisions or initiations

Authors

Gabriele Micali, Jacopo Grilli, Jacopo Marchi, Matteo Osella, Marco Cosentino Lagomarsino

Correspondence

marco.cosentino-lagomarsino@ifom.eu

In Brief

The current paradigm assumes that *E. coli* cell division occurs a fixed time after DNA replication, but recent single-cell studies reached contrasting conclusions on this. By model-guided data analysis, Micali et al. falsify the classic assumption and test mechanistic scenarios for concurrent processes competing to determine cell division.

Micali et al., 2018, Cell Reports *25*, 761–771
October 16, 2018
https://doi.org/10.1016/j.celrep.2018.09.061

CellPress

Cell Reports
Article

Dissecting the Control Mechanisms for DNA Replication and Cell Division in *E. coli*

Gabriele Micali,[1,2,11] Jacopo Grilli,[3,10,11] Jacopo Marchi,[4] Matteo Osella,[5,6] and Marco Cosentino Lagomarsino[7,8,9,12,*]
[1]Department of Environmental Microbiology, Eawag, Dübendorf, Switzerland
[2]Department of Environmental Systems Science, ETH Zürich, Zürich, Switzerland
[3]Santa Fe Institute, 1399 Hyde Park Road, Santa Fe, NM 87501, USA
[4]Laboratoire de Physique Théorique, Département de Physique, École Normale Supérieure, PSL, Sorbonne Universités, UPMC Université Paris 06, CNRS, 75005 Paris, France
[5]Physics Department, University of Turin, Via Giuria 16, Torino, Italy
[6]I.N.F.N., Torino, Italy
[7]Sorbonne Universités, UPMC Univ. Paris 06, Paris, France
[8]CNRS, UMR 7238, Paris, France
[9]IFOM, FIRC Institute of Molecular Oncology, Milan, Italy
[10]The Abdus Salam International Centre for Theoretical Physics (ICTP), Strada Costiera 11, 34014 Trieste, Italy
[11]These authors contributed equally
[12]Lead Contact
*Correspondence: marco.cosentino-lagomarsino@ifom.eu
https://doi.org/10.1016/j.celrep.2018.09.061

SUMMARY

Understanding the classic problem of how single *E. coli* cells coordinate cell division with genome replication would open the way to addressing cell-cycle progression at the single-cell level. Recent studies produced new data, but the contrast in their conclusions and proposed mechanisms makes the emerging picture fragmented and unclear. Here, we re-evaluate available data and models, including generalizations based on the same assumptions. We show that although they provide useful insights, none of the proposed models captures all correlation patterns observed in data. We conclude that the assumption that replication is the bottleneck process for cell division is too restrictive. Instead, we propose that two concurrent cycles responsible for division and initiation of DNA replication set the time of cell division. This framework allows us to select a nearly constant added size per origin between subsequent initiations as the most likely mechanism setting initiation of replication.

INTRODUCTION

Each cell needs two copies of the genome to divide. The notion that this simple principle must be central for the cell cycle was already clear in early studies (Meselson and Stahl, 1958; Nurse et al., 1998). For the model organism *E. coli*, a wealth of information was gathered starting from the late 1950s (Cooper and Helmstetter, 1968; Donachie, 1968; Schaechter et al., 1958, 1962), leading to important insights about cell-cycle progression. Today, a relevant set of the key molecules playing a role in the cell cycle of these bacteria is known (Adams and Errington, 2009; Cho et al., 2011; Donachie, 1993; Donachie and Blakely, 2003; Egan and Vollmer, 2013; Hill et al., 2013; Lutkenhaus et al., 2012). However, determining how cell division is coordinated with genome replication in *E. coli* is still an open problem. The reason is that our knowledge is still based mostly on population averages, which mask the behavior of single cells (Osella et al., 2017). Instead, understanding homeostatic processes in cell-cycle progression needs the knowledge of correlations between subsequent cell-cycle events at the single-cell level. For example, we do not know for sure whether replication initiation is triggered at a critical size in single cells (Ho and Amir, 2015; Osella et al., 2017; Wallden et al., 2016), whether there are licensing constraints inhibiting initiations (Bates and Kleckner, 2005; Osella et al., 2017), and whether the rate-limiting checkpoint for the decision to divide is typically independent from replication initiation (Harris and Theriot, 2016).

A wave of experimental and theoretical studies promises to untie this knot, because high-throughput, single-cell data are becoming routinely available (Campos et al., 2014; Hashimoto et al., 2016; Iyer-Biswas et al., 2014; Jun and Taheri-Araghi, 2015; Kennard et al., 2016; Kiviet et al., 2014). These measurements can in principle access the full correlation pattern of several cell-cycle events, from which we can extract mechanistic interpretations (Osella et al., 2017). For instance, there is agreement that in most cases, the added volume between consecutive cell divisions is nearly uncorrelated with cell size at birth, a principle sometimes called adder (Adiciptaningrum et al., 2015; Amir, 2014; Campos et al., 2014; Harris and Theriot, 2016; Osella et al., 2017; Soifer et al., 2016; Taheri-Araghi et al., 2015; Wallden et al., 2016). However, fundamentally different models that account for this adder behavior have been proposed (Adiciptaningrum et al., 2015; Harris and Theriot, 2016; Ho and Amir, 2015; Osella et al., 2017; Wallden et al., 2016), leaving us with a complex landscape of models that appear to be incompatible and to contrast one another. Additionally, we lack a general theoretical

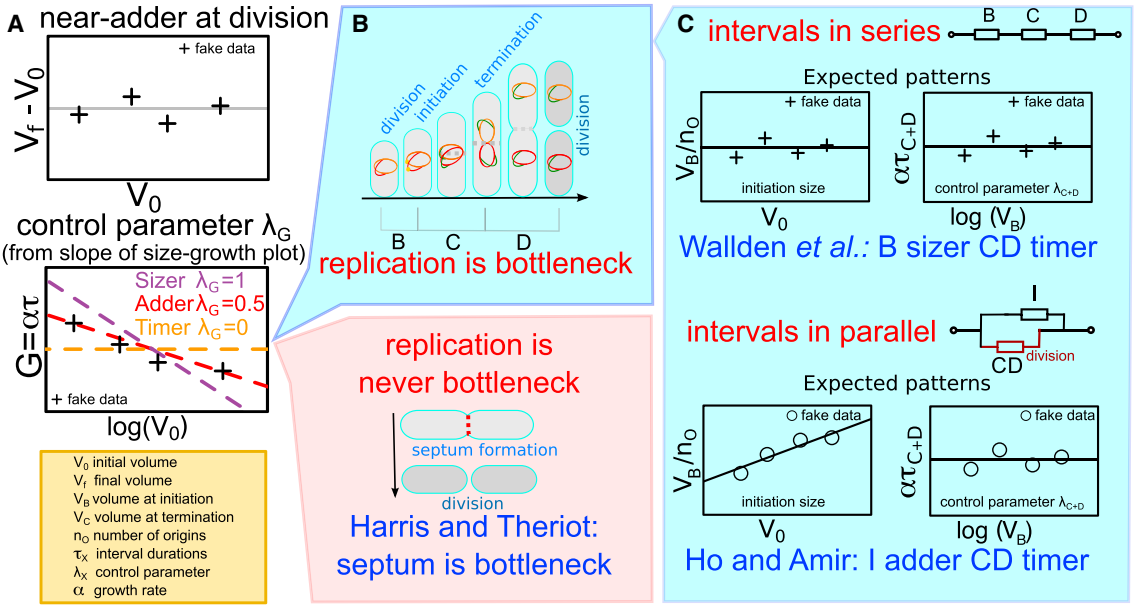

Figure 1. Comparison of the Existing Models Linking Cell-Cycle Progression to Cell Division in Single *E. coli* Cells

(A) Top: all models need to comply to the robust near-adder pattern found in data (added size over the cell cycle uncorrelated with initial size). Middle: near-adder pattern in the size-growth plot of net growth $G = \log(V_f/V_0) = \alpha\tau$ versus logarithmic initial size $\log(V_0)$ with a negative slope of 1/2. The slope parameter λ_G between 0 (no control) and 1 (absolute threshold) quantifies size control. Bottom: definition of main variables (see Table S1).

(B) Opposite hypotheses for cell division. Top: completion of replication and segregation is always rate limiting (Ho and Amir, 2015; Wallden et al., 2016). Bottom: it is never limiting, and division may be triggered by, e.g., a threshold amount of surface material necessary to form the septum (Harris and Theriot, 2016).

(C) Models in which replication and segregation is the bottleneck. The cartoon plots summarize the expectation, in each model, for correlation patterns between the volume at birth V_0 and the size at initiation per origin V_B/n_O (left plot) and between $\alpha\tau_{C+D}$ and logarithmic initiation size $\log V_B$, where τ_{C+D} is the period between replication initiation and division (right plot). Top: Wallden et al. (2016) assume that the periods associated with replication and segregation are consecutive and juxtaposed in series. This model postulates a critical size per origin at initiation and a duration of τ_{C+D} that is coupled to single-cell growth rate, but not to cell size. Bottom: in the Ho-Amir model (Ho and Amir, 2015), the timing between initiation and division τ_{C+D} and that between subsequent initiations τ_I run in parallel from a single initiation event. Only τ_I is coupled to size in a way that a constant size per origin is added between successive initiations.

framework to interpret the correlation patterns in the data and to compare and falsify different models.

Here, we aim to provide a solid framework for solving the apparent contradictions among recent claims by a joint modeling and data analysis approach (considering the available high-quality, single-cell datasets). Focusing on the coordination of genome replication with cell division, we start by reanalyzing available data and models. In a parallel study, we introduced the concurrent-cycles idea: a division-related process (e.g., completion of the septum) and a replication-segregation process (e.g., release of occlusion from the nucleoid) compete to set cell division (Micali et al., 2018). In this study, we develop this idea in two directions. First, we systematically study general models based on the two alternative hypotheses that replication is always or never the limiting process for division. Despite the flexibility and the additional free parameters of these general models compared with the ones proposed in the literature, we show that they irremediably lead to predictions that are inconsistent with available data if the whole pattern of correlations is considered. Second, assuming the concurrent-cycles framework, we ask whether it is possible to capture all measured correlation patterns and to use them to isolate the specific mechanisms setting initiation and division, focusing on scenarios in which the concurrent processes work on already proposed mechanisms for the interdivision and interinitiation processes, such as adders or sizers.

RESULTS

Review of Current Models of the *E. coli* Cell Cycle

We start by reviewing available models and the key differences in their predictions (Figure 1) that need to be reconciled. As a premise, all models must reproduce the ubiquitous near-adder correlation pattern, robustly found for cell division in several datasets (Jun and Taheri-Araghi, 2015), i.e., that added size between consecutive initiations is uncorrelated with initial size (Figure 1A).

Harris and Theriot (2016) assume (Figure 1B) that the process of replication and segregation is never the bottleneck process for cell division, because it is typically completed well in advance, before other rate-limiting processes trigger division. They also propose that of the multiple checkpoints needed for cells to complete division, the one that is rate limiting could be the accumulation of a target surface material (enough to build the septum). Under this assumption, and further assuming that surface synthesis rate is proportional to cell volume, one finds near-adder correlations (Supplemental Experimental Procedures).

A main assumption of this model is that genome replication and segregation is typically faster than the critical accumulation of the factor triggering division and thus that cell division can be unaware of the chromosomes. Studies measuring how different perturbations affect mean cell size conclude that this is not

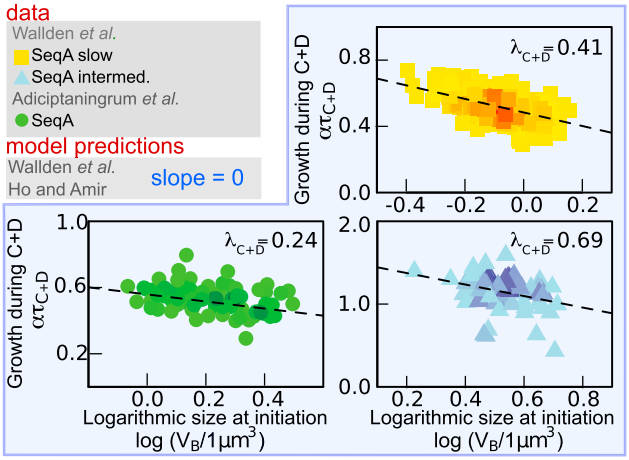

Figure 2. Current Models Fail to Capture the Experimental Correlation Patterns of the Cell-Cycle Intervals Related to Replication and Segregation ($C+D$ Period)

Scatterplot and slope of the size-growth plot for the $C+D$ period, i.e., $\alpha\tau_{C+D}$ as a function of initiation size $\log(V_B)$. Data from Wallden et al. (2016) show slow (yellow squares) and intermediate (light blue triangles) growth conditions, and data from Adiciptaningrum et al. (2015) are shown as green circles. All datasets presented were obtained by labeling SeqA molecules. The negative values of the slopes (dashed lines from linear fits of binned data), quantifying the parameters λ_{C+D}, robustly show size-coupled growth during the $C+D$ period.

generally the case (Si et al., 2017; Zheng et al., 2016), but work by Harris and Theriot (2016) does not address the evidence pointing to a link between replication and cell division (Donachie, 1968; Donachie and Blakely, 2003). Thus, in the best-case scenario, it needs to be complemented with a description of DNA replication.

The prevalent view, assumed by all other available models, is that instead, the bottleneck process for division is the completion of replication and segregation. We focus specifically on the link between replication and cell division (Figures 1B and 1C). In this case, the cell cycle is naturally divided into the B, C, D periods defined by replication initiation, duration of replication, and cell division (Figure 1B) and analogous to the G1, S, and G2/M periods of eukaryotic cell cycles.

In particular, two main models are used to explain cell division based on the idea that the replication and segregation process is rate limiting. Both models are based on the assumption that cell division takes place at a size-independent time after initiation of replication, but they differ in how replication initiation is controlled. A model by Ho and Amir (2015) assumes that cells add a constant size (i.e., independent from the cell size at initiation) per origin between initiations (adder between initiations), while division is set by a constant time $C+D$ (timer) after initiation. A competing model by Wallden et al. (2016) proposes that initiation is triggered by a constant cell size per origin, while cell division can phenomenologically resemble a sizer or a near-adder, depending on the growth conditions (more details later). This sizer per origin extends to single cells the classic picture (Donachie, 1968, 1993) that assumes a sizer at initiation, motivated by population-averaged data (Osella et al., 2017). Both models are compatible with this constant average size per origin at initiation and thus with empirical observations at the population level. However, from a single-cell perspective, the assumption of a critical size per origin is radically different from the assumption of a constant added mass since the last initiation event. There are open questions of whether and how the available data suffice to distinguish between these two alternative scenarios.

Invalidation of Current Models Based on the $C+D$ Correlation Patterns

We have shown in a parallel study (Micali et al., 2018) that the existing models cannot capture correlation patterns in the $C+D$ period. This section recapitulates these inconsistencies between data and model predictions in more detail. For each model describing the replication-division cycle, Figure 1C shows two key predicted correlation patterns for the B and $C+D$ period. First, the volume per origin at initiation V_B versus initial volume V_0 tests the existence of a size threshold for initiation in single cells. This plot has zero slope if a size threshold exists (a sizer, i.e., control parameter $\lambda_B = 1$). Second, the correlation pattern between the growth in the $C+D$ period $\alpha\tau_{C+D}$ and the initial size tests a possible coupling between replication-segregation cell-cycle interval and cell size. The slope of this plot is zero if the $C+D$ period is uncoupled from size (a timer, i.e., control parameter $\lambda_{C+D} = 0$).

The contrasting Ho-Amir and Wallden et al. models agree in the claim that there is no control between initiation and division, $\lambda_{C+D} = 0$ (Figure 1C), but the duration of this period fluctuates around a cell size-independent value (a timer). A third study by Adiciptaningrum et al. (2015) found experimentally that the duration of the D period, the time between termination of replication and cell division, was anticorrelated with the size at the termination of replication. This coupling between D period duration and cell size is at odds with the assumptions of both models. This pattern is confirmed by data from Wallden et al. (2016), as shown in Figure 2, and the existing models where on replication and segregation are the rate-limiting process for division do not reproduce it. In addition, the assumption that DNA replication is never a bottleneck, as in the Harris-Theriot model (Harris and Theriot, 2016), leads to quantitatively wrong predictions in the single-cell correlation patterns of the replication-related cell-cycle intervals. We discuss this question in more detail later, because this model represents a specific limiting case of the concurrent-cycles framework.

To further explore the limitations of the classic hypothesis that division is limited by replication and segregation, we introduce two classes of models that generalize the two descriptions by Ho-Amir and by Wallden and coworkers. These generalizations show that the assumption of replication and segregation as the single rate-limiting process for division leads to predictions that cannot be reconciled with empirical data, even when the correlation pattern in Figure 2 is captured with *ad hoc* ingredients.

Definition of Generalized Models Based on Replication and Segregation as the Rate-Limiting Process for Division

We define a general modeling framework that assumes that replication-segregation "bottlenecks" cell division, with the

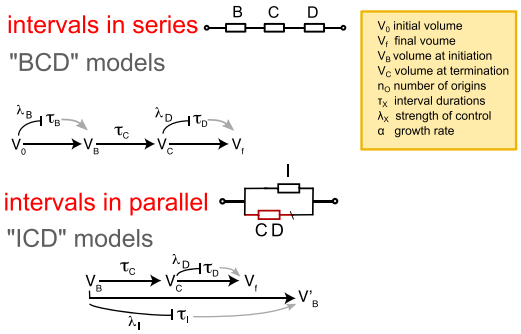

Figure 3. Scheme of the Generalized Models BCD and ICD

General schemes of models in series (BCD, see also Adiciptaningrum et al., 2015) and in parallel (ICD). In the sketches, each model is characterized by the control parameters λ_X coupling growth during a cell-cycle interval and cell size. Noise parameters in each model describe the variability of each cell-cycle interval at a fixed initial size.

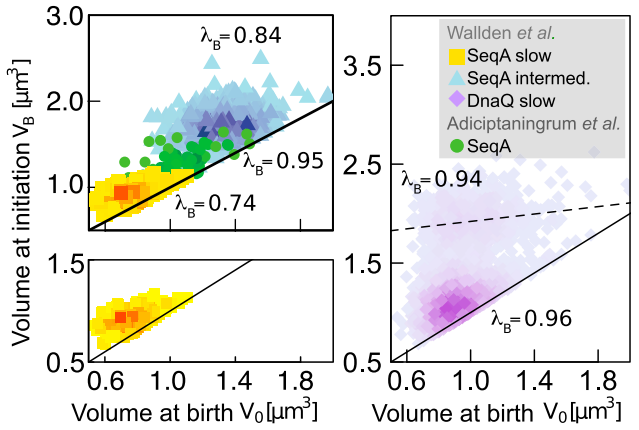

Figure 4. Inconclusive Empirical Evidence for a Sizer at Initiation

Volume at initiation versus birth volume. SeqA data from Wallden et al. (2016) show slow (yellow squares) and intermediate (light blue triangles) growth conditions, and SeqA data from Adiciptaningrum et al. (2015) are shown as green circles. Color scales correspond to the probability density (see Supplemental Information). The solid line has a slope of 1 (V_B = V_0). The bottom-left and bottom-right panels show the same plot using SeqA and DnaQ labeling data, respectively, in the same slow-growth conditions (data from Wallden et al., 2016). Data from DnaQ show the possibility of a second initiation per cell cycle (see Supplemental Experimental Procedures section S1). Conversely, SeqA foci are detected only after division (Osella et al., 2017). The weak dependency of the size of the second initiation and initial size (dashed line is the slope from the binned average) is only loosely consistent with a sizer (secondary initiations are extracted from foci subcellular localization, tracking, and cell size) (Figure S1). The annotated values of λ_B are extracted from the equivalent size-growth plots (Figure S2) by Bayesian fits, taking into account the constraints.

scope of highlighting the limitations of this assumption. The two models by Ho-Amir and by Wallden and coworkers fundamentally differ in the assumption of how the cell-cycle intervals corresponding to the B, C, D periods are temporally juxtaposed (see the sketches in Figure 1C). In the model by Wallden and coworkers, the cell-cycle intervals are placed in series, and no interval can begin if the previous one is not completed. Conversely, in the Ho-Amir model, there is an overarching interval connecting subsequent initiations, and the interval corresponding to the $C+D$ period runs in parallel. Thus, the B period in this model is a result of the two parallel cell-cycle intervals (their difference is in the absence of overlapping replication rounds).

Therefore, we consider two general wiring diagrams of couplings between size and growth (Figure 3), which we call ICD (in parallel) and BCD (in series). In these general schemes, each cell-cycle interval is drawn as an arrow, and the size is coupled to the duration of the interval by generic parameters. These parameters can represent controls acting in case of a size fluctuation, e.g., by reducing the duration of the period in case the cell is larger than average at entry. Each cell-cycle interval is characterized by the coupling parameter λ_X between its duration and its cell size (e.g., volume). Such parameters are evaluated directly from the size-growth plots of relative growth during each interval versus initial size (illustrated in Figure 1A) and may range from 0 (timer, no control) to 1 (sizer, absolute size threshold).

Specifically, we aim to show that in models assuming that replication is always bottleneck, even parametric generalizations, which are in principle more flexible (Adiciptaningrum et al., 2015), lead to predictions that deviate from data.

Indecisive Evidence for a Critical Size Threshold at Replication Initiation from Direct Measurements

Before addressing the models, we need to review the experimental support in single cells for the assumption of a sizer at initiation. Clear evidence for a size threshold at initiation would limit the parameter space of our generalized models. Therefore, we reanalyzed the available data to test the correlation patterns in the B period and to compare them to model predictions or assumptions. Figure 4 summarizes the results of this analysis.

As noted previously (Osella et al., 2017; Wallden et al., 2016), data on replication initiation obtained by labeling SeqA molecules show a constraint whereby foci appearance is recorded only when $V_B > V_0$. This constraint is visible in Figure 4 as a cut in the correlation clouds between initial volume V_0 and volume at initiation V_B. The cut cloud is because of unrecorded initiation events in the previous cell cycle (which is typically not available or tracked in the dataset). To estimate the slopes in the presence of the constraint, we performed a Bayesian fit of a bivariate Gaussian using the data in Figure 4 under the assumption that the data below the constraint were censored (see Supplemental Experimental Procedures for a description and testing of this algorithm). The results are not far from a sizer, but they also deviate sensibly from this pattern.

DnaQ foci are more visible before division, although these data are affected by false-positive detection because of blinking and by poor segmentation tracking of cells (Wallden et al., 2016). Despite of these problems, the DnaQ data show evidence of double initiations in the same cell cycle and allow a different analysis, because the data of secondary initiations are free from the cut in the correlation cloud. Secondary initiations can occur in cells with delayed divisions (which might meet the size criteria for initiation twice in the same cell cycle). We have performed a refined analysis of the B period in the DnaQ data, defining secondary initiations from information on foci subcellular localization and time tracks of both foci and cell size (see Supplemental Experimental Procedures and Figure S1).

Figure 4 shows the cell volume at initiation V_B against the cell volume at birth V_0 (not shown in the Wallden et al., 2016, study). We conclude the following. First, at the same range of volumes at birth, a secondary cloud of initiations at large volumes appears for DnaQ. The reasons why such double initiations are not visible with SeqA are unclear, but we believe they are likely biological, because SeqA foci do not blink and are more stable and visible than DnaQ foci (Adiciptaningrum et al., 2015; Osella et al., 2017; Wallden et al., 2016). This may relate to previous observations leading to the licensing hypothesis for initiation (Bates and Kleckner, 2005; Kleckner et al., 2018). Second, correlation in the secondary cloud of Figure 4 confirms the idea that initiation size is weakly correlated with birth size, generally close to but slightly divergent from the pattern expected from a sizer. However, because of blinking, we consider DnaQ data to be less reliable than SeqA for the primary cloud of initiations. This is because mother-daughter progression is not tracked, and as a consequence, it is not possible to reliably assign initiation to the first cloud, because the appearance of foci early in the cell cycle could be because of a real initiation or a blinking event in the mother cell.

In conclusion, the available direct measurements of initiation size do not conclusively point to the presence of a size threshold at initiation and generally show a weak but noticeable positive correlation of initiation size with birth size.

Inconsistencies between Measured Correlation Patterns for the *B* and *C* + *D* Periods and Generalized Models

Having reviewed the main experimental correlations, we go back to the generalized models of Figure 3 to analyze whether they may reproduce them. Specifically, we asked whether the observed correlation patterns in the $C+D$ period (Figure 2) and in the B period (Figure 4) could be reproduced jointly and consistently by these models (see Supplemental Experimental Procedures sections S4 and S5 and Figure S4).

A non-zero control variable λ_{C+D} coupling initiation size to division (such as the one that is built in the Adiciptaningrum et al., 2015, model) can be added in a straightforward way to any model. This would trivially make the models able to reproduce the correlation trends in $C+D$ (Figure 2), although this extra parameter does not have a natural interpretation.

We then considered the B period. An issue raised by Figure 4 is the question of how adder correlations between divisions can be compatible with a scenario in which initial volume and initiation volume are at most weakly correlated. In particular, if we assume an adder between initiations, we need to explain the weak correlation between initiation size and birth size. However, we found that in the presence of noise, the ICD model (and thus the Ho-Amir model as a particular case) can predict low correlations between initial size and initiation size (and hence high λ_B) (see Supplemental Experimental Procedures and Figure S4). Therefore, the correlation pattern in the B period (Figure 4) is not sufficient to distinguish between the models, and one has to consider other observables (see Supplemental Experimental Procedures section S6 and Figure S5).

The failure of the entire framework emerges when the patterns for the B and $C+D$ periods are considered jointly. To further test whether the ICD and BCD models could be consistent with data, we solved them analytically, obtaining consistency relationships among the different control parameters. The main relationships are shown in Box 1. These mathematical expressions are valid in the approximation in which the number of overlapping rounds does not fluctuate, but they agree well with simulations (Figure S6). Although in both ICD and BCD models, one is allowed to tune the control parameter λ_{C+D} between replication initiation and corresponding division event, both models have to follow a general relationship between the interdivision control parameter λ_G (Figure 1A) and the product of the B period and $C+D$ period parameters, $(1-\lambda_G)^n = (1-\lambda_B)\cdot(1-\lambda_{C+D})$, where n is the number of overlapping replication rounds (Box 1; Supplemental Experimental Procedures section S6 and Figure S6). In addition, this relationship does not depend on the noise levels, unlike the one relating the interdivision and the interinitiation patterns (Box 1). Thus, it is expected to be robust in the data. This relationship is verified in simulations (Figure S6), but Figure 5 indicates that the data are in disagreement. This analysis leads us to suggest that the strict assumption that replication is the sole bottleneck for cell division leads to inconsistencies with data.

Sizer Theorem: If Any Subperiod Is in Series with a Sizer, Interdivision Time Is a Sizer

To fully show that existing models based on the hypothesis that replication-segregation is the limiting step for cell division fail, we need to deal separately with the model proposed by Wallden and coworkers (Wallden et al., 2016), which is based on some specific assumptions that transcend the ICD and BCD framework. One of the main reasons for the failure of the ICD and BCD frameworks shown in Figure 5 is that the size control of the B period affects the control between divisions. A consequence of this could be termed the sizer theorem: a near-sizer at initiation (witnessed by weak correlation between initial size and initiation size), as well as in any cell-cycle interval in the chain of events leading to cell division, leads to near-sizer correlations between subsequent divisions. This fact, shown by simulations in Figure 6A, is simple to derive theoretically, because once cell-cycle progression hits a sizer (and hence a trigger that is uncorrelated with the initial size of the previous subperiod), memory of all previous sizes is lost; hence, the division size will be uncorrelated with the initial size (Soifer et al., 2016).

Therefore, any model assuming a sizer at initiation has to bypass the sizer theorem to be compatible with near-adder correlations between subsequent divisions. We proceed to show how the model proposed by Wallden and coworkers solves this problem, but we also show that this solution leads to predictions that are falsified by the available data.

The Wallden et al. Model Escapes the Sizer Theorem because of Correlations across Generations and Stochasticity of Single-Cell Growth Rates

Wallden et al. (2016) simulate a model in which initiation is triggered by a sizer, compatible with our reanalysis of their experimental data and Figure 4. However, the interdivision correlations in this model are not compatible with a sizer, violating the sizer theorem (Figure 6A). To explain how this is possible, the authors argue with simulations that the result is because of a direct

Box 1. Relations between the Control Parameters of Different Cell-Cycle Intervals in Different Models

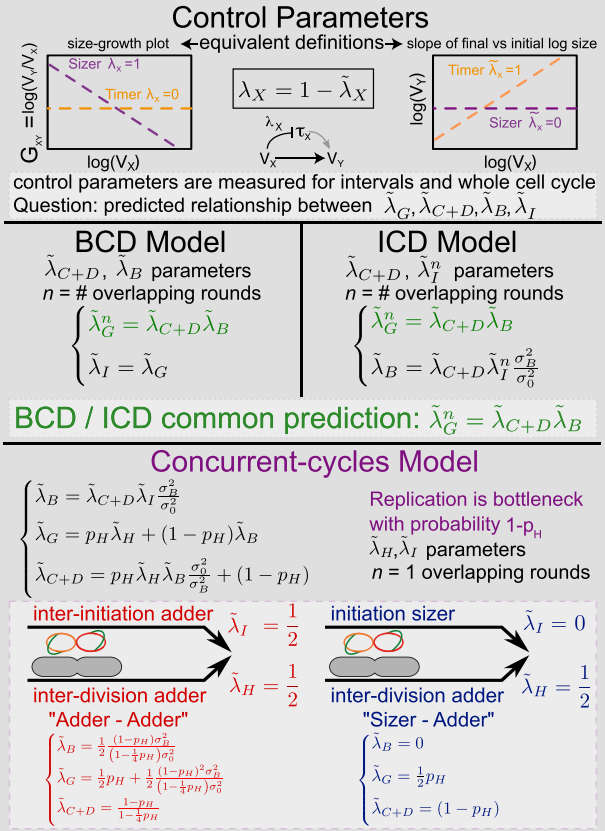

Top: equivalent definitions of control parameters (see also Figure S2). The control parameters λ_X (extracted from the slope of size-growth plot as in the sketch) and $\tilde{\lambda}_X$ (the slope of the scatterplot of the logarithmic size at the end versus the beginning of the cell-cycle interval) can be used equivalently. Different models predict different relationships among the control parameters measured on all cell-cycle intervals. Middle: main relations between control parameters for the BCD and those for the ICD models. These general models in which the chromosome cycle is rate limiting lead to the same common prediction (in green) linking the product of the control parameters of the *B* and *C* + *D* periods ($\tilde{\lambda}_B$ and $\tilde{\lambda}_{C+D}$, respectively) to the overall interdivision control parameter $\tilde{\lambda}_G$. Bottom: main relations for the concurrent-cycles model. In these formulas, p_H is the probability that the interdivision cycle is bottleneck ($p_H \simeq 0.6$ if the size scales encoded by the two concurrent processes are matched). The red and blue brackets show the key particular cases of adder between divisions concurring with adder between initiations and sizer at initiation, respectively.

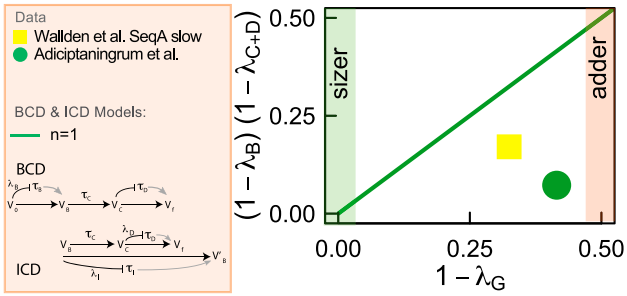

Figure 5. Discrepancy of Data with General Models Assuming that Replication-Segregation Is the Bottleneck Process for Cell Division

The plot tests the relationship between the predicted size control of consecutive divisions and the observed correlation patterns for the *B* and *C* + *D* periods. For both the BCD and the ICD models (Box 1), this is predicted to be an identity in absence of overlapping rounds. This prediction is matched by simulations (Figure S6) but is violated in data for the two available conditions in the absence of overlapping rounds, casting doubts on both models even in their parameter-flexible formulations.

growth-rate dependency of *C* + *D* period duration to growth rate (Figure 6B), which they fit empirically from data with a power law. The direct link between this feature and the model behavior is not clarified in their work, nor is the reason for the near-inverse relationship between the single-cell growth rate and the duration of the *C* + *D* period, which is taken as an empirical fact. Because of this coupling, the authors argue that the sizer at initiation can translate to different mechanisms at division because of the coupling of *C* + *D* duration to single-cell growth. In particular, they show that this can lead to the near-sizer correlation patterns between divisions measured in their data for slow-growth conditions, which become closer to a near-adder for fast-growth conditions.

To shed light on this result, we introduce an equivalent parameter-poor model, in which a simpler set of ingredients leads to the same behavior without the need for arbitrary phenomenological fitting procedures. Specifically, we assume (Figure 6B) that (1) initiation is driven by a sizer as in the standard version of the model, (2) the *C* period is a timer, and (3) the *D* period is a grower, i.e., the net growth quantified by $\alpha D = \log(V_f/V_D)$ is uncorrelated with size at replication termination $\log(V_D)$. This last ingredient is different from a simple timing mechanism. It implies that, e.g., in cells where α is larger, the *D* period duration will tend to be shorter; hence, the two variables in the product $G_D = \alpha\tau_D$ become naturally anticorrelated. Conversely, if it were a timer, the net growth would be still uncoupled from the initial size, but the fluctuations of the subperiod duration would not be coupled to single-cell growth rate.

The assumed grower correlations for the *D* period lead to define a model that behaves equivalently to the model of Wallden and coworkers, with the advantage that the coupling of *C* + *D* period duration with growth rate is not adjusted by hand but rather is a natural consequence of the grower assumption. We were able to solve this model analytically for the interdivision correlation patterns, revealing the explanation of the effect found by Wallden et al. (2016), and we compared it with simulations and empirical data.

Our prediction is that growth-rate correlations (quantified by Pearson correlation ρ) across generations give rise to a correlation loss in the interdivision size-growth plot with respect to the

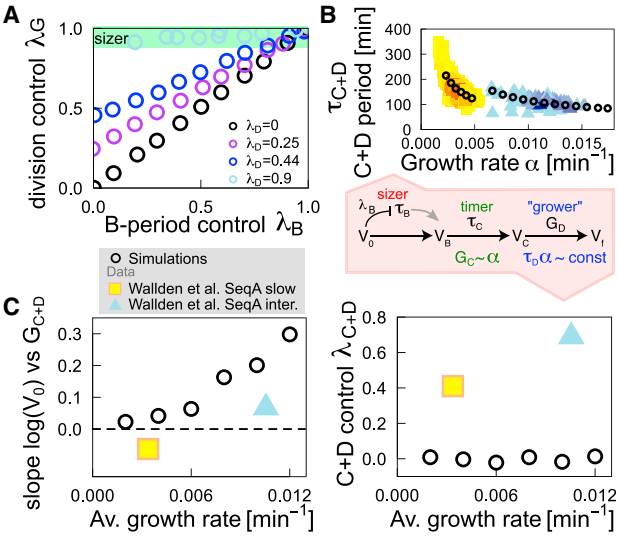

Figure 6. Mother-Daughter Correlations Bypass the Sizer Theorem, but the Resulting Model Is Still in Contrast to Available Data

(A) Sizer theorem: if any cell-cycle interval is a sizer and intervals are placed in series, then the interdivision correlation pattern is a sizer. The division cycle control λ_G is plotted as a function of the growth control parameter λ_B for the *B* period in the BCD model. The division control increases with increasing control over the *B* period and *D* period ($\lambda_D = 0$ black, $\lambda_D = 0.25$ purple, $\lambda_D = 0.44$ blue, and $\lambda_D = 0.9$ light blue circles). In particular, a sizer at replication initiation implies a sizer on the division cycle, regardless the level of control on the *D* period.

(B) Model in which the *B* period is a sizer, *C* is a timer, and *D* is a grower (see main text), similar to the model in Wallden et al. (2016). This model incorporates the observed trend between individual-cell growth rate and $C+D$ period duration as a consequence of the timer+grower pattern.

(C) Resulting model is at odds with the Wallden et al. data. The correlation between the logarithmic size at birth and the growth during the $C+D$ period (left panel) is predicted to be positive (circles correspond to simulations) but is close to zero in the data (filled symbols) from Wallden et al. (2016). Conversely (right panel), the size control parameter during the $C+D$ periods is predicted to be zero (circles), while experimental data clearly deviate from this value (filled symbols).

Parameters: (A) Simulations are performed by varying λ_B while keeping fixed the noise ratio $\sigma_{C+D}/\sigma_{B+C+D} = 0.7$. The other parameters are inferred from data from Adiciptaningrum et al. (2015): $\alpha = 0.0053$ min^{-1}, $\langle t_B \rangle = 30$ min, $\langle t_C \rangle = 78$ min, $\langle q_0 \rangle = 0.03$, and $\langle n \rangle = 1$. (B–C) Average growth rates range from 0.002 to 0.012 min^{-1}, with a constant coefficient of variation (CV) equal to 0.2. Mother-daughter correlation of growth rate is set at $\rho = 0.5$. In this modified Wallden et al. model, the average *C* period is set to 42 min, with CV 0.1, and for the grower period, $\alpha\tau_D$ is set to be 0.6 on average, with CV 0.1. The experimental values for the Wallden et al. slow-growth condition (yellow squares) are ≈ -0.06 and 0.41 for (C) in the left and right panel, respectively. The experimental values for the Wallden et al. intermediate-growth condition (light blue triangles) are ≈ 0.06 and 0.69 for (C) in the left and right panel, respectively. The average size per origin at initiation is set to $\nu = 0.9[\mu m^3]$, with a constant CV of 0.1 for all panels.

sizer. We also predict that an analogous effect is expected in the presence of overlapping replication rounds because of the correlations induced by a *C* period lasting multiple generations (Figure S3). The mechanism is as follows. A cell that grows at faster rate than average will typically divide at a larger size. The growth rate of the subsequent generation will thus retain a memory of the initial size (through its correlation with the growth rate of the previous generation). Because the $C+D$ period is relying partly on a timer and partly on a grower, its anticorrelation with the growth rate will create an effective correlation of its duration with the initial, not the initiation, size and hence weaken the sizer correlation between divisions (see Supplemental Information for a full explanation and calculation).

This prediction is in line with the arguments provided by Wallden et al. (2016), and it is in excellent agreement with simulations. Unfortunately, the agreement is unsatisfactory when compared with empirical data from several published studies of interdivision correlation patterns (Figure S3).

Crucially, these ingredients do not produce the correct correlation patterns for the $C+D$ period (Figure 6C). The Wallden et al. model, as well as our variant (which is equivalent), predict that there should be (negative) correlation between initial cell size and growth during the $C+D$ period but no correlation between initiation size and growth during the $C+D$ period. The former is a consequence of the memory effect carried by the persistence of the individual cell growth rate and the timer+grower pattern of the $C+D$ period, while the latter is a consequence of loss of memory of the initial size at initiation given by the sizer mechanism (sizer theorem). Figure 6C shows that empirical data from the Wallden et al. (2016) study follow the opposite pattern, showing stronger correlations between $C+D$ period duration and initiation size and weaker correlations between $C+D$ period duration and birth size.

Thus, although we have provided a simple rationale for the model proposed by Wallden and coworkers, and we support the observations that lead to its definition, we can conclude that the basic ingredients of this model cannot be fully correct.

A Concurrent-Cycles Model Based on Competition between Adders Explains the Correlation Patterns from Simple Ingredients

All preceding considerations give a fairly complete account of the problems encountered by trying to explain available data with models that assume that replication and segregation is always a bottleneck for cell division. In particular, these models fail to capture crucial features of the $C+D$ period (Figure 2) or the composite pattern of correlations among *B*, *C* + *D*, and the overall cell cycle (Figure 5).

We use this knowledge to pinpoint the size-regulatory processes in the concurrent-cycles framework (Micali et al., 2018). In this model, competition between two concurrent processes, one setting division and one controlling initiation of DNA replication, naturally reproduces the pattern in Figures 2 and 6B without *ad hoc* assumptions or additional parameters (Micali et al., 2018). The basic idea is to relax the hypothesis that replication-segregation is always the bottleneck process and assume that concurrent cycles regulate division and the replication-segregation cycle. In other words, the model assumes that neither the limit where the bottleneck process is always chromosome segregation (Adiciptaningrum et al., 2015; Ho and Amir, 2015; Wallden et al., 2016) nor the limit where segregation typically finishes before division (Harris and Theriot, 2016) are realized.

Although a concurrent-processes scenario is supported by analyses that are independent on the specific control mechanisms (Micali et al., 2018), once we assume this framework, it

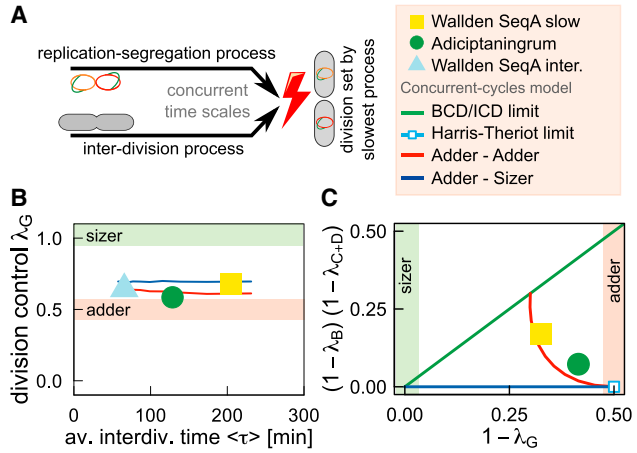

Figure 7. Correlation Patterns of the Concurrent-Cycles Model Fully Agree with Available Data and Support the Hypothesis of a Near-Adder per Origin between Initiations

(A) Schematic of the concurrent-cycles model: an interdivision process and a process setting replication initiation compete for the decision of the cell to divide. We considered the cases in which an adder between divisions concurs with an adder between initiations (red lines) or a sizer at initiation (blue lines).

(B) The division control parameter λ_G as a function of the average interdivision time gives a near-adder for both concurrent models, in agreement with data. The predictions assume that there is not a clear separation of the size scales of the two processes ($p_H \sim 0.5$) and thus that competition between processes is present.

(C) Comparison of empirical data (without overlapping replication rounds) with the predictions of the adder-adder versus sizer-adder models allows selection of the mechanism setting initiation. The green lines correspond to models based on replication-segregation as the single rate-limiting process for cell division (BCD and ICD models). The limit case (light blue, corresponding to the Harris-Theriot hypothesis or $p_H \simeq 1$) of a chromosome-agnostic division also fails to reproduce the data. Only the concurrent-cycles model with an adder between consecutive initiations and an interdivision adder (red line corresponding to a noise ratio of σ_B^2/σ_0^2 fixed from data) can match the data by varying the only free parameter, p_H (the probability that replication is not the bottleneck in a cell cycle), in a relatively narrow range around 0.5 ($p_H = [0.25, 0.75]$), compatible with our assumption of competition between two processes. Numerical simulations and data with overlapping replication rounds are shown in Figure S7.

remains important to identify the most likely mechanisms. As we have shown, empirical data leave open the question of the control of replication initiation (Figure 4). Hence, we used the concurrent-cycles framework, in combination with the available data, to pinpoint the most likely mechanism setting replication initiation. Following Harris and Theriot (2016) (and as suggested by several empirical observations; see Figure 1A), we started by assuming that the interdivision process is a near-adder. We then compared two variants in which initiation is set by a sizer per origin (sizer-adder scenario) or by an adder per origin (adder-adder scenario) between subsequent initiation events, and we asked whether the correlation patterns in the available data are sufficient to distinguish these scenarios.

After each initiation, a minimum (size uncoupled) $C+D'$ period is necessary before division. D' may not be the observed duration of the D period when the completion of the replication-segregation period is not the bottleneck event for cell division. The slowest of the two concurrent processes decides division (Figure 7A).

An important quantity in this model is the probability p_H that the interdivision process is the limiting one. This parameter is an output of the model and depends on both concurrent processes. It is related to the typical added size between divisions and its variability for the interdivision process, as well as to the typical size at initiation and duration of the $C+D'$ period in the replication-related cycle.

The concurrent-cycles framework only relies on parameters that are fixed from data or from natural assumptions and are not forcedly adjusted. The control parameters of the two concurrent processes λ_I and λ_H are fixed *a priori* by the specific assumed mechanisms for the concurrent cycles, as in previous models (we considered the cases of adder-adder and sizer-adder) (Box 1). An additional timescale (or equivalently, a size scale) needs to be defined in this framework. Specifically, this timescale is captured by the parameter D', and depending on its relation to the natural timescale of the system set by the doubling time, it will define which of the two processes is more likely to be the slowest (i.e., the value of p_H). Equivalently, the two size scales associated with the processes correspond to the mean size per origin at initiation, which several studies indicate is constant in different conditions (Si et al., 2017; Zheng et al., 2016), and to the average added size. However, to have the two concurrent processes in competition, their associated time or size scales have to be comparable, and this condition fixes a narrow range for the parameter D' and consequently for p_H.

Under the assumption that the two time (or size) scales are comparable, both model variants have a comparable number of parameters as (or fewer parameters than) the Ho-Amir and Wallden et al. models, and they robustly give a near-adder correlation pattern across divisions (Figure 7B), with a slight deviation from the pure-adder prediction ($\lambda_G = 0.5$), which is compatible with the data. In addition, we have shown (Micali et al., 2018) that both model variants naturally capture the correlation patterns relative to the $C+D$ period (Figures 2 and 6B) without the need to add these trends as *a priori* ingredients.

The model gives different predictions (Box 1), depending on the model assumptions, for the relationships among the control parameters λ_B, λ_{C+D}, and λ_G. These plots allow testing of the process regulating replication initiation by the correlation patterns of the concurrent-cycles model (Box 1). We find that the datasets coherently support the assumption of an adder per origin between subsequent initiations (Ho and Amir, 2015). Because the control parameters of the model are all fixed by the hypothesis that the interdivision and interinitiation processes are both near-adders, and the noise parameters can be fixed directly from data, the only parameter that is allowed to vary in these models is p_H. We verified that empirical data can be captured by varying this parameter in a relatively narrow range of values around 0.5. This supports the idea that the timescales of the two processes are approximately matched and thus competition is typically in place. In addition, a comparison of these predictions with the empirical data (Figure 7C; Figure S7) confirms the limitations of existing models and their generalizations. In particular, the extreme case of replication and segregation as a bottleneck (BCD and ICD limit, corresponding to $p_H = 0$)

fails regardless of the flexibility of the parameters, and the same is true for the opposite limit (Harris-Theriot limit, $p_H = 1$).

DISCUSSION

What Is the Bottleneck Process for Cell Division?

As clearly explained by previous studies (Harris and Theriot, 2016; Ho and Amir, 2015; Osella et al., 2017), a central point in solving the question of the determinants of cell division in *E. coli* is whether the process of replication followed by segregation is a bottleneck for cell division. The more conventional view (Ho and Amir, 2015; Wallden et al., 2016) is that the chromosome cycle is always a bottleneck and that the decision to divide is slaved to the decision to initiate replication through the processes of completing replication and segregation. The strongest pieces of evidence in this direction are classic and recent observations on mean cell size, which we discuss later. The less conventional hypothesis of Harris and Theriot (2016), motivated by their measurements of the mean surface and volume dynamics of *E. coli* cells, is that replication is never a bottleneck for cell division. Under this assumption, *E. coli* decides to divide independently of the chromosome replication cycle.

Our main result is twofold. First, a wide class of models based on a single rate-limiting process setting cell division is unable to explain at the same time the correlation patterns for the cell-cycle subperiods. This failure of the replication-based models (Ho and Amir, 2015; Wallden et al., 2016) points to a model in which replication is not always bottleneck but two (or more) processes, of which (at least) one is replication related, act on similar timescales and compete for setting cell division (Micali et al., 2018). Second, assuming this framework of concurrent cycles, our analysis clearly indicates that replication initiation is set by a near-adder per origin between initiations, as suggested by Ho and Amir (2015) (described later).

One outstanding question is whether the concurrent-cycles scenario could be relevant to other species. This is a testable hypothesis using the tools developed here and in Micali et al. (2018). To our knowledge, the only published dataset in which this is possible is the one by Logsdon et al. (2017) in mycobacteria. The authors of this work assume that the chromosome cycle is rate limiting for cell division and conclude that an ICD-like model in which the $C+D$ period control is a near-adder is the most likely scenario.

The Peculiar Nature of the *D* Period

The principal reward of the concurrent-cycles framework is to robustly explain two puzzling trends found in the $C+D$ period and not accounted for by the current literature: (1) $C+D$ period duration is anticorrelated with single-cell growth rate with a near-inverse pattern, and (2) the amount of growth during this period is anticorrelated with cell size (Micali et al., 2018).

It is important to spell out how these ingredients lead to problems in existing models. Wallden et al. (2016) need to fit the duration of the $C+D$ period to a power law with a variable offset and exponent without justification. In addition, they have to assume large mother-daughter correlations in the growth rate, and our analysis (Figure 6; Figure S3) shows that the measured growth-rate correlations do not justify the observed patterns. In addition, although all models can incorporate a size-coupled $C+D$ period (nonzero λ_{C+D}) as an extra ingredient, this ingredient does not have a natural explanation, and we have shown how this choice still leads to problems with the data when the B and $C+D$ periods are considered jointly (Figure 5).

We also stress that the basic ingredient of our model, i.e., concurrence between two synchronous cycles, is different from the hypothesis of parallel subperiods of previous models (Ho and Amir, 2015; Logsdon et al., 2017) that basically can be assimilated to the ICD framework presented here. In all these models, only one replication-related process (the $C+D$ period) sets division and runs in parallel with another process (the I period) setting the interinitiation time. By contrast, in the concurrent-cycles formalism, cell division can be controlled by the slower of two processes, only one of which is related to replication.

A consequence of concurrent cycles is that the D period has a peculiar status, because its duration is subject to the joint control of both concurrent processes. Consequently, this period is the result of multiple processes, including (1) a minimum time from termination to division necessary to complete segregation (at a given growth condition) in case the replication-related process triggers division and (2) the additional residual time necessary to wait for the completion of the interdivision process in case this process is the slowest one and determines division. This suggests an adaptable duration for the D period depending on the size reached at termination (Osella et al., 2017).

Size Control at Replication Initiation

Our analysis supports the conclusion that the correlation of initiation size and initial size is not negligible, at least in some datasets. To draw this conclusion, we reanalyzed the SeqA data available in the literature, as well as the DnaQ data from Wallden et al. (2016). In agreement with these authors, we find that secondary initiations are possible. By performing this analysis, we show that in this data, initiation size may carry some weak but noticeable positive correlation with initial size. In addition, the occurrence of double initiations, on theoretical grounds, is necessary to restore steady conditions from a perturbation. For example, suppose that a cell misses a replication initiation event. It will then need a double initiation to align its size and chromosome content to the average of its population. Therefore, it seems more plausible that the SeqA behavior is more because of some specific property of this molecule than a symptom of a constraint on replication initiation.

Setting this question aside, and assuming that the correlation pattern of the observed points is meaningful, we developed an algorithm to score correlations for clouds of points cut by known constraints, allowing information to be extracted on the real correlation between volume at initiation and initial volume from the SeqA datasets from Wallden et al. (2016), removing the spurious correlations arising from points being available only for the initiation volumes larger than the volume at birth. In addition, in this case, we detected weak but significant positive correlations.

Both the ICD model and the concurrent-cycles model show that the weak correlation observed between initial size and initiation size does not necessarily point to sizer control. The same correlation pattern can be found in the scenario of an adder (or a different control) between subsequent initiations. In a

framework of concurrent cycles, the reason for this is that the correlation between the two variables, initial size and initiation size, is decreased by the possibility that the two different processes decide division.

Overall, comparing the concurrent-cycles model with data, and considering all observed correlation patterns jointly, a scenario of adder control between subsequent initiations appears to be the most plausible (Figure 7; Figure S7). It is remarkable that the model can make this prediction even though data analysis cannot directly settle this point. In the future, direct measurements of added volume between subsequent initiations will likely settle this point directly.

Tuning of the Size Scale of the Competing Circuits

Two auxiliary pieces of evidence are important. First, two studies measured changes in cell size under several genetic and molecular perturbations affecting key variables such as metabolism, replication, synthesis of essential cell components, and cell-cycle proteins (Si et al., 2017; Zheng et al., 2016). Assuming that initiation triggers cell division after an average constant time, the $C+D$ period, both studies conclude that on average, cells initiate replication at a critical size per origin (Si et al., 2017; Zheng et al., 2016), as hypothesized classically by Donachie (1968) (Cooper, 1993; Cooper and Helmstetter, 1968; Schaechter et al., 1962). This is only one of two possible causal links, and an independently set cell size could govern the timing of initiation. However, in this scenario, it would be harder to explain the near-exponential dependency of mean cell size from mean growth rate found across conditions and valid under several perturbations (Donachie, 1968; Micali et al., 2018; Schaechter et al., 1958; Si et al., 2017; Vadia et al., 2017; Zheng et al., 2016). Second, cell sizes show scaling, and a single size scale defines the probability distribution of initial (at birth) sizes and interdivision times (Kennard et al., 2016; Taheri-Araghi et al., 2015). In other words, the histograms of these variables collapse (across conditions) when rescaled by their means. These two facts indicate that the cell cycle encodes a unique size scale for the cells and that this scale corresponds to the average size per origin at initiation. Because size is set by the decision to divide, this means either that a single rate-limiting process typically decides cell division (Harris and Theriot, 2016) or that if multiple processes act on similar timescales, they need to be tuned in a way that their characteristic size and timescales coincide. In addition, these processes have to be informed about (or inform) the origin number or genome amount.

The concurrent-cycles assumption is meaningful if typically there is competition between the two concurrent processes. This means that in a given condition, cells have a non-negligible (and non-small) probability of dividing with either of the concurrent processes. For this to be the case, the intrinsic size scales of the two processes (mean added size between divisions and mean size at initiation) have to be comparable (and proportional). Any limit for which only one process dominates simply reduces to the previously available models (Amir, 2017; Harris and Theriot, 2016; Wallden et al., 2016) and makes our formalism redundant. The matching or near-matching between the two size scales is also a necessary consequence of the existence of a single size scale determining the probability distribution of cell size in *E. coli* (Kennard et al., 2016; Taheri-Araghi et al., 2015).

Targeted perturbations of the cell cycle may also support the hypothesis that these scales are matched. For example, deletion of SlmA, the nucleoid occlusion protein preventing *E. coli* cells from dividing in the presence of unsegregated chromosomes, leaves mean cell size unaffected (Bernhardt and de Boer, 2005; Cho et al., 2011). We interpret this as a clue in favor of self-tuning of the intrinsic size scale of the interdivision process and the size scale set by replication initiation. Because the two concurrent processes may not compete (or compete less) in these mutants, our prediction is that looking at the behavior of single cells, the size distribution and the size-timing correlation patterns of these mutants should differ from the wild-type.

Finally, competition between concurrent cycles could explain why *E. coli* cells growing at extremely slow rates deviate from adder correlations. This could come from variations in the frequency at which each process is a bottleneck (p_H in our model). We also observe that even in the presence of adder control, both between subsequent initiations and between subsequent divisions, the concurrent-cycles model at matched size scales gives a stronger control between division than does an adder (in line with data) (Grilli et al., 2018).

STAR★METHODS

Detailed methods are provided in the online version of this paper and include the following:

- KEY RESOURCES TABLE
- CONTACT FOR REAGENT AND RESOURCE SHARING
- METHOD DETAILS
  - Datasets
  - Models
- QUANTIFICATION AND STATISTICAL ANALYSIS
- DATA AND SOFTWARE AVAILABILITY

SUPPLEMENTAL INFORMATION

Supplemental Information includes Supplemental Experimental Procedures, seven figures, and one table and can be found with this article online at https://doi.org/10.1016/j.celrep.2018.09.061.

ACKNOWLEDGMENTS

We thank Sven van Teeffelen, Clotilde Cadart, Bianca Sclavi, Ilaria Iuliani, Ariel Amir, Po Yi Ho, Nancy Kleckner, and Sander Tans for helpful feedback on this work. This work was supported by an International Human Frontier Science Program Organization grant (HFSP RGY0070/2014). M.O. was supported by the "Departments of Excellence 2018–2022" grant awarded by the Italian Ministry of Education, University and Research (MIUR) (L. 232/2016). J.G. was supported by an Omidyar Postdoctoral Fellowship at the Santa Fe Institute. G.M. was supported by a grant (31003A_169978) from the Swiss National Science Foundation to Martin Ackermann.

AUTHOR CONTRIBUTIONS

M.C.L., M.O., G.M., and J.G. designed the study. G.M. coordinated the numerical and data analysis work; G.M., J.G., and J.M. performed data analysis and simulations. J.G. coordinated the analytical work on the models; J.G., J.M., M.C.L., and G.M. performed analytical calculations. M.C.L. conceived and

managed the project and wrote the paper; all authors provided feedback and help on the writing.

DECLARATION OF INTERESTS

The authors declare no competing interests.

Received: May 29, 2018
Revised: August 22, 2018
Accepted: September 19, 2018
Published: October 16, 2018

REFERENCES

Adams, D.W., and Errington, J. (2009). Bacterial cell division: assembly, maintenance and disassembly of the Z ring. Nat. Rev. Microbiol. *7*, 642–653.

Adiciptaningrum, A., Osella, M., Moolman, M.C., Cosentino Lagomarsino, M., and Tans, S.J. (2015). Stochasticity and homeostasis in the *E. coli* replication and division cycle. Sci. Rep. *5*, 18261.

Amir, A. (2014). Cell size regulation in bacteria. Phys. Rev. Lett. *112*, 208102.

Amir, A. (2017). Is cell size a spandrel? eLife *6*, e22186.

Bates, D., and Kleckner, N. (2005). Chromosome and replisome dynamics in *E. coli*: loss of sister cohesion triggers global chromosome movement and mediates chromosome segregation. Cell *121*, 899–911.

Bernhardt, T.G., and de Boer, P.A. (2005). SlmA, a nucleoid-associated, FtsZ binding protein required for blocking septal ring assembly over chromosomes in *E. coli*. Mol. Cell *18*, 555–564.

Campos, M., Surovtsev, I.V., Kato, S., Paintdakhi, A., Beltran, B., Ebmeier, S.E., and Jacobs-Wagner, C. (2014). A constant size extension drives bacterial cell size homeostasis. Cell *159*, 1433–1446.

Cho, H., McManus, H.R., Dove, S.L., and Bernhardt, T.G. (2011). Nucleoid occlusion factor SlmA is a DNA-activated FtsZ polymerization antagonist. Proc. Natl. Acad. Sci. USA *108*, 3773–3778.

Cooper, S. (1993). The origins and meaning of the Schaechter-Maaløe-Kjeldgaard experiments. J. Gen. Microbiol. *139*, 1117.

Cooper, S., and Helmstetter, C.E. (1968). Chromosome replication and the division cycle of *Escherichia coli* B/r. J. Mol. Biol. *31*, 519–540.

Donachie, W.D. (1968). Relationship between cell size and time of initiation of DNA replication. Nature *219*, 1077–1079.

Donachie, W.D. (1993). The cell cycle of *Escherichia coli*. Annu. Rev. Microbiol. *47*, 199–230.

Donachie, W.D., and Blakely, G.W. (2003). Coupling the initiation of chromosome replication to cell size in *Escherichia coli*. Curr. Opin. Microbiol. *6*, 146–150.

Egan, A.J.F., and Vollmer, W. (2013). The physiology of bacterial cell division. Ann. N Y Acad. Sci. *1277*, 8–28.

Grilli, J., Osella, M., Kennard, A.S., and Lagomarsino, M.C. (2017). Relevant parameters in models of cell division control. Phys. Rev. E *95*, 032411.

Grilli, J., Cadart, C., Micali, G., Osella, M., and Cosentino Lagomarsino, M. (2018). The empirical fluctuation pattern of *E. coli* division control. Front. Microbiol. *9*, 1541.

Harris, L.K., and Theriot, J.A. (2016). Relative rates of surface and volume synthesis set bacterial cell size. Cell *165*, 1479–1492.

Hashimoto, M., Nozoe, T., Nakaoka, H., Okura, R., Akiyoshi, S., Kaneko, K., Kussell, E., and Wakamoto, Y. (2016). Noise-driven growth rate gain in clonal cellular populations. Proc. Natl. Acad. Sci. USA *113*, 3251–3256.

Hill, N.S., Buske, P.J., Shi, Y., and Levin, P.A. (2013). A moonlighting enzyme links *Escherichia coli* cell size with central metabolism. PLoS Genet. *9*, e1003663.

Ho, P.Y., and Amir, A. (2015). Simultaneous regulation of cell size and chromosome replication in bacteria. Front. Microbiol. *6*, 662.

Iyer-Biswas, S., Wright, C.S., Henry, J.T., Lo, K., Burov, S., Lin, Y., Crooks, G.E., Crosson, S., Dinner, A.R., and Scherer, N.F. (2014). Scaling laws governing stochastic growth and division of single bacterial cells. Proc. Natl. Acad. Sci. USA *111*, 15912–15917.

Jun, S., and Taheri-Araghi, S. (2015). Cell-size maintenance: universal strategy revealed. Trends Microbiol. *23*, 4–6.

Kennard, A.S., Osella, M., Javer, A., Grilli, J., Nghe, P., Tans, S.J., Cicuta, P., and Cosentino Lagomarsino, M. (2016). Individuality and universality in the growth-division laws of single *E. coli* cells. Phys. Rev. E *93*, 012408.

Kiviet, D.J., Nghe, P., Walker, N., Boulineau, S., Sunderlikova, V., and Tans, S.J. (2014). Stochasticity of metabolism and growth at the single-cell level. Nature *514*, 376–379.

Kleckner, N.E., Chatzi, K., White, M.A., Fisher, J.K., and Stouf, M. (2018). Coordination of growth, chromosome replication/segregation, and cell division in *E. coli*. Front. Microbiol. *9*, 1469.

Logsdon, M.M., Ho, P.-Y., Papavinasasundaram, K., Richardson, K., Cokol, M., Sassetti, C.M., Amir, A., and Aldridge, B.B. (2017). A parallel adder coordinates mycobacterial cell-cycle progression and cell-size homeostasis in the context of asymmetric growth and organization. Curr. Biol. *27*, 3367–3374.

Lutkenhaus, J., Pichoff, S., and Du, S. (2012). Bacterial cytokinesis: From Z ring to divisome. Cytoskeleton (Hoboken) *69*, 778–790.

Meselson, M., and Stahl, F.W. (1958). The replication of DNA in *Escherichia coli*. Proc. Natl. Acad. Sci. USA *44*, 671–682.

Micali, G., Grilli, J., Osella, M., and Cosentino Lagomarsino, M. (2018). Concurrent processes set *E. coli* cell division. bioRxiv. https://doi.org/10.1101/301671.

Nurse, P., Masui, Y., and Hartwell, L. (1998). Understanding the cell cycle. Nat. Med. *4*, 1103–1106.

Osella, M., Tans, S.J., and Cosentino Lagomarsino, M. (2017). Step by step, cell by cell: quantification of the bacterial cell cycle. Trends Microbiol. *25*, 250–256.

Schaechter, M., Maaløe, O., and Kjeldgaard, N.O. (1958). Dependency on medium and temperature of cell size and chemical composition during balanced grown of *Salmonella typhimurium*. J. Gen. Microbiol. *19*, 592–606.

Schaechter, M., Williamson, J.P., Hood, J.R., Jr., and Koch, A.L. (1962). Growth, cell and nuclear divisions in some bacteria. J. Gen. Microbiol. *29*, 421–434.

Si, F., Li, D., Cox, S.E., Sauls, J.T., Azizi, O., Sou, C., Schwartz, A.B., Erickstad, M.J., Jun, Y., Li, X., and Jun, S. (2017). Invariance of initiation mass and predictability of cell size in *Escherichia coli*. Curr. Biol. *27*, 1278–1287.

Soifer, I., Robert, L., and Amir, A. (2016). Single-cell analysis of growth in budding yeast and bacteria reveals a common size regulation strategy. Curr. Biol. *26*, 356–361.

Taheri-Araghi, S., Bradde, S., Sauls, J.T., Hill, N.S., Levin, P.A., Paulsson, J., Vergassola, M., and Jun, S. (2015). Cell-size control and homeostasis in bacteria. Curr. Biol. *25*, 385–391.

Vadia, S., Tse, J.L., Lucena, R., Yang, Z., Kellogg, D.R., Wang, J.D., and Levin, P.A. (2017). Fatty acid availability sets cell envelope capacity and dictates microbial cell size. Curr. Biol. *27*, 1757–1767.

Wallden, M., Fange, D., Lundius, E.G., Baltekin, Ö., and Elf, J. (2016). The synchronization of replication and division cycles in individual *E. coli* cells. Cell *166*, 729–739.

Zheng, H., Ho, P.-Y., Jiang, M., Tang, B., Liu, W., Li, D., Yu, X., Kleckner, N.E., Amir, A., and Liu, C. (2016). Interrogating the *Escherichia coli* cell cycle by cell dimension perturbations. Proc. Natl. Acad. Sci. USA *113*, 15000–15005.

STAR★METHODS

KEY RESOURCES TABLE

REAGENT or RESOURCE	SOURCE	IDENTIFIER
Deposited Data		
Datasets for cell cycle information (e.g., single cell growth rate, volume at birth, initiation and division) about the DnaQ- and SeqA-labeled strains in the slow, intermediate and fast conditions.	Wallden et al., 2016	http://elflab.icm.uu.se/references/Wallden_et_al_2016.zip
Datasets with cell cycle information (e.g., single cell growth rate, length at birth, initiation and division) about the SeqA-labeled strains.	Adiciptaningrum et al., 2015	N/A
Datasets with cell length at birth and division, single cell growth rate for couple of mother-daughter cells and for five different experimental conditions.	Kennard et al., 2016	N/A
Datasets with cell length at birth and division, single cell growth rate for couple of mother-daughter cells and for five different experimental conditions.	Taheri-Araghi et al., 2015	https://jun.ucsd.edu/mother_machine.php
Software and Algorithms		
Software to reproduce the data available. The file includes code for BCD and ICD models, for the generalized Wallden model and for the concurrent cycle models adder – adder and adder – sizer cases.	This paper	https://data.mendeley.com/datasets/zwpyxk3fwk/draft?a=4cbab8a5-1226-4a5e-9ebe-2497773806fb

CONTACT FOR REAGENT AND RESOURCE SHARING

Further information and requests for reagents should be directed to the Lead Contact, Marco Cosentino Lagomarsino (marco.cosentino-lagomarsino@ifom.eu).

METHOD DETAILS

Datasets

We used published datasets from refs. (Adiciptaningrum et al., 2015; Kennard et al., 2016; Taheri-Araghi et al., 2015; Wallden et al., 2016).

The data from refs.(Adiciptaningrum et al., 2015; Wallden et al., 2016) contain information on replication initiation and cell division on tracked single cells, and constitute the core of our analysis. The dataset from ref. (Adiciptaningrum et al., 2015) was obtained directly from the authors. The dataset from ref. Wallden et al. (2016) was downloaded online at http://elflab.icm.uu.se/references/Wallden_et_al_2016.zip. The analysis presented here focuses on the slow growth condition only. The file '' DnaQ_pooled_per_molecule_slow_data.txt'' contains information about single cell growth (time since birth, volume, length and width) and (whenever it is detected) the number and the position of fluorescently labeled epsilon subunit of DNA polymerase (Pol) III, named DnaQ, which is a proxy for replication forks Wallden et al. (2016). In order to measure the correlations between the volume at birth and initiation, we used the tracking data provided by the authors. These data are noisy, and some assumptions are needed to identify the initiations. First, we filtered the dataset checking that the cells were tracked with time intervals below 3.5 minutes, that the volume at initiation was not lower than the volume at birth and not higher than the volume at division (thus correcting for tracking errors). We further filtered out volume changes higher than 0.2 μm^3 during a time step, to correct for non-biological negative or extremely fast growth, mostly due to tracking errors. In order to identify likely initiation events, we considered the 3111 single cells that show at least one fluorescent focus, and used joint information on foci appearance and subcellular localization, and cell size (the results of this analysis are described in detail in Supplemental Experimental Procedures, section S1).

The other data (from refs. (Adiciptaningrum et al., 2015; Kennard et al., 2016; Taheri-Araghi et al., 2015; Wallden et al., 2016)) only contain growth-division data of tracked single cells and were used for further comparisons of models' predictions with data (these datasets were collected and analyzed in ref. Grilli et al. (2018)).

Models

Models were analyzed by both direct simulations and analytical calculations.

We considered and analyzed different stochastic models for the cell cycle at the single-cell level. These analyses can be divided into three stages: (i) a re-analysis of the published models in refs. (Ho and Amir, 2015; Wallden et al., 2016) (ii) the generalizations and formulations of the models of refs. (Ho and Amir, 2015; Wallden et al., 2016), called "ICD" and "BCD" frameworks, and (iii) the concurrent-cycle model proposed in (Micali et al., 2018). We focus mainly on the special case where the inter-division process is an adder, which has as a limit case when replication is never a bottleneck the pure adder model advocated by ref. (Harris and Theriot, 2016), and we consider the two alternatives of a sizer at initiation ("sizer-adder" model) or an adder per origin ("adder-adder" model) for the inter-initiation process. Our analytical results are presented in Supplemental Experimental Procedures (sections S4 and S5).

BCD models

The BCD framework is defined by the assumption that the replication-related cell-cycle subperiods are in series, and one interval can only start when the previous one is complete. In absence of overlapping rounds, the volume at division V_f is given by

$$V_f = V_0 \exp(\alpha t_B + \alpha t_C + \alpha t_D), \tag{1}$$

where the growth rate α is assumed here to be constant (but we also considered the case where it is a random variable), and t_X is the time spent during the sub-cycle X.

The times t_X are random variable with some dependence on the cell-size, we assume a linear dependency and describe the controls of different sub-cycles using a single parameter. Under these assumptions the three different sub-period times can then be written:

$$t_B = \langle t_B \rangle - \frac{\lambda_B}{\alpha}(q_0 - \langle q_0 \rangle) + \nu_B \tag{2}$$

$$t_C = \langle t_C \rangle - \frac{\lambda_C}{\alpha}(q_B - \langle q_B \rangle) + \nu_C \tag{3}$$

$$t_D = \langle t_D \rangle - \frac{\lambda_D}{\alpha}(q_C - \langle q_C \rangle) + \nu_D \tag{4}$$

where $\langle t_X \rangle$ is the mean duration of the sub-period, ν_X represents the noise, q_0 is the natural logarithm of the size at birth, and q_X is the natural logarithm of the size at the end of sub-period X. Finally, the parameters λ_X define the strength of size control. The higher is λ_X, the more the corresponding subperiod duration is anti-correlated with the size at the beginning of the period. A value $\lambda_X = 0$ corresponds to a timer, while $\lambda_X = 1$ is a sizer Amir (2014); Grilli et al. (2017). Note that, contrarily to what happens for the whole cell-cycle, $\lambda_X = 1/2$ does not correspond to a near-adder for the sub-period X. Figure 2 in the main text outlines the presented model and its ingredients, illustrating the meaning of the parameters.

The model of Wallden and coworkers assumptions is a BCD model where the single-cell growth rate is a random variable and there are correlated growth-rate fluctuations. Specifically, the main assumptions are that (i) sizer at initiation, i.e., $V_B = V_0 \exp(\alpha t_B) = \tilde{V}\exp(\xi_B)$, where $\tilde{V}$ is a constant size and ξ_B is a random noise with mean zero independent of V_0, (ii) the C period is a timer, i.e., $t_C = \tau_C + \zeta_C$, where τ_C is a constant and ζ_C is a random noise with mean zero independent of V_0 and V_B and (iii) the D period is a grower, i.e., $\alpha t_D = d^* + \xi_D$, where d^* is a constant independent of the other variables, and ξ_D is a random noise with mean zero, independent of V_0, V_B and V_C. Note that ξ_B and ξ_D are dimensionless while ζ_C has dimensions of time.

ICD models

ICD models consider the cell cycle as composed by three intervals: "I" (between consecutive initiations), "C" (DNA replication), and "D" (from termination of DNA replication to cell division), which are **not** in series, since the I and C+D period run in parallel starting from replication initiation.

The defining equations, for constant growth rate and in absence of overlapping rounds in the same notation as above, are

$$t_I = \langle t_I \rangle - \frac{\lambda_I}{\alpha}(q_B - \langle q_B \rangle) + \nu_I \tag{5}$$

$$t_C = \langle t_C \rangle - \frac{\lambda_C}{\alpha}(q_B - \langle q_B \rangle) + \nu_C \tag{6}$$

$$t_D = \langle t_D \rangle - \frac{\lambda_D}{\alpha}(q_C - \langle q_C \rangle) + \nu_D. \tag{7}$$

The model by Ho and Amir Ho and Amir (2015) can be seen as a specific ICD model assuming that the added size (per origin) between consecutive initiations is constant and does not depend on size fluctuations. This model corresponds to an ICD model with $\lambda_D = 0$ (and $\lambda_I = 1/2$).

Concurrent-cycles models

In concurrent cycles models, cell division is determined by the slowest of a cell-related inter-division process and a chromosome-related inter-initiation process. In absence of overlapping rounds, the interdivision process is similar to the model proposed Harris and Theriot. This process is concluded at a log-size q_H, which is simply

$$q_H = q_H^* + (1 - \lambda_H)\left(q_0 - \left(q_H^* - \log 2\right)\right) + \alpha\eta_H, \tag{8}$$

where λ_H is an inter-division control parameter setting size control.

The chromosome process sets cell division completed at a log-scale q_R

$$q_R = q_R^* + \delta q_B + \alpha\eta_R, \tag{9}$$

where

$$q_R^* = \langle q_R \rangle = \langle q_B \rangle + \alpha\tau_{C+D'}, \tag{10}$$

and $\tau_{C+D'}$ is the time needed to complete replication and segregation.

The actual division event, hence the cell size at division, is determined by the slowest process, i.e.

$$q_f = \max(q_H, q_R). \tag{11}$$

QUANTIFICATION AND STATISTICAL ANALYSIS

Coupling parameters between growth in a cell-cycle interval and size (the parameters λ_X in our models) were evaluated from scatterplots as linear fits of binned averages ('lm' function in R based on least-squares), or alternatively (the parameters $\tilde{\lambda}_X$) from the equivalent method based on the covariance of two variables (Box 1; Supplemental Experimental Procedures, section S4). The two methods are equivalent, but binned averages have the advantage of estimating efficiently the conditional averages defining the control parameters in presence of high noise (Grilli et al., 2017). Error bars in all our plots are smaller than symbol sizes.

The analysis reconstructing the size correlation secondary initiations in the DnaQ datasets from Wallden et al. (Wallden et al., 2016) is based on selecting secondary initiations by subcellular position and cell size if initiation events. Figure S1 shows that initiations are localized in clusters in a time-space diagram. Cross-analysis of the clusters with the time series of foci appearance allows to filter cells where two initiations appear early and late in the cell cycle (see Supplemental Experimental Procedures, sec. S1, and Figure S1 for the results).

In presence of constraints, i.e., for initiations that were scored in the data only after division, we performed a Bayesian fit of a bivariate Gaussian keeping the constraint into account, and extracted the control parameters λ_X from the covariance (see Figure S2). Let (x, y) be a pair of random variables, we suppose that we can only observe a pair (x, y) if $y > x$. Hence, the actual distribution $p_c(x, y)$ one sampling from is

$$p_c(x, y) = \frac{1}{Z}\Theta(y - x)p(x, y), \tag{12}$$

where the original distribution is assumed to be Gaussian,

$$p(x, y) = \frac{1}{\sqrt{2\pi \det\Sigma}} \exp\left(-\frac{1}{2}\left(x - \mu_x, y - \mu_y\right)\Sigma^{-1}\left(x - \mu_x, y - \mu_y\right)^t \right), \tag{13}$$

and

$$\Sigma = \begin{pmatrix} \sigma_x^2 & \rho\sigma_x\sigma_y \\ \rho\sigma_x\sigma_y & \sigma_y^2 \end{pmatrix} \tag{14}$$

is the covariance matrix. $\Theta(\cdot)$ is the Heaviside theta function, Z is a normalization factor. Assuming that the observations $\{(x_1, y_1), (x_2, y_2), \ldots, (x_N, y_N)\}$ meet the constraint $y_i > x_i$ for all the i, the log-likelihood reads

$$\begin{aligned} \log \mathcal{L} = & -N \log Z - \frac{N}{2}\log\left(2\pi\left(1 - \rho^2\right)\sigma_x\sigma_y\right) + \\ & -\frac{1}{2(1 - \rho^2)}\sum_i \left(\frac{(x_i - \mu_x)^2}{\sigma_x^2} + \frac{(y_i - \mu_x)^2}{\sigma_y^2} + \frac{(x_i - \mu_x)(y_i - \mu_y)}{\sigma_x\sigma_y} \right). \end{aligned} \tag{15}$$

Note that the normalization factor Z can also be interpreted as the probability that a random pair (x, y) drawn from the distribution $p(x, y)$ meet the constraint $y > x$. Z does therefore depend, in a non-trivial way, on the parameters. Since this dependence cannot be expressed analytically, we maximized the likelihood numerically, by calculating numerically the value of Z for each proposed new combination of parameters. The algorithm was tested on computational data (Supplemental Experimental Procedures, section S2).

DATA AND SOFTWARE AVAILABILITY

The custom-written code (made of several programs and scripts in C,C++, python and R) generated for statistical analysis and model simulation is available at the following link: https://data.mendeley.com/datasets/zwpyxk3fwk/draft?a=4cbab8a5-1226-4a5e-9ebe-2497773806fb.